J Therm Anal Calorim (2010) 102:155–162
DOI 10.1007/s10973-010-0995-2

Thermal infrared mapping of the freezing phase change activity of micro liquid droplet

F. F. Li · J. Liu

Received: 8 April 2010 / Accepted: 30 July 2010 / Published online: 18 August 2010

Abstract This article is dedicated to develop an experimental approach for directly visualizing the global freezing phase change behavior of micro liquid droplets. The infrared (IR) thermograph was proposed to image the basic solidification phenomena of droplet and to acquire its temperature variations during the transient process. In particular, the volumetric recalescence event, regarded as initiation of freezing, was revealed by IR images for the first time. Preliminary results demonstrated that the involved temperature transition due to release of the latent heat can be accurately characterized by evident color break in IR images. Further, experiments were also performed simultaneously on three kinds of droplets made of pure water, dimethylsulfoxide (DMSO) and nano liquid to grasp more precise temporal and spatial temperature distribution. Types of the occurring solidification and the initial frozen volume produced from the recalescence were generally discussed. The IR monitoring method suggests a straightforward way for detecting the freezing phase change activity and its temperature evolution at micro scale.

Keywords Freezing phase change · Liquid droplet · Thermal infrared mapping · Micro/nanofluids

F. F. Li · J. Liu (✉)
Key Laboratory of Cryogenics,
Technical Institute of Physics and Chemistry,
Chinese Academy of Sciences, Beijing 100190,
People's Republic of China
e-mail: jliu@mail.ipc.ac.cn

J. Liu
Department of Biomedical Engineering,
School of Medicine, Tsinghua University,
Beijing 100084, People's Republic of China

Introduction

As one of the most popular and crucial issues, freezing phenomenon has attracted much public interest for many years. It was believed that clarity of the freezing mechanism would be of great significance for both fundamental sciences and engineering applications. The physical and chemical properties of the liquid have received much attention because of their important influence on solidifying process. Up to now, typical works have been focused in the fields of meteorology, food engineering, cryobiomedicine, etc. [1–4]. For example, in the climatic systems, traditional thermodynamic theory was applied for prediction of hail or snowfall [5], since freezing is often depicted as a thermal and kinetic process of a new phase creation via nucleation and subsequent crystal growth from supercooled water [6]. The nucleation process, which determines whether the final freezing will happen, is always regarded as the most critical factor. In cryobiomedical field, freezing acts as either a protector or a destroyer of the biological tissues. Accomplishment of the contrary purposes is highly reliant on the cooling program, which is usually regarded as the decisive factor for final fate of the cells. According to the classical Mazur's model [7], it is the freezing rate that determines whether the cell injury is attributed by the intracellular ice formation or cell dehydration. Besides, there also exist other effects such as the restricted space, the solution effect, the interaction between cells and the external electrical or magnetic field, etc. impacting on the freezing process at molecular or cellular scale. Along with the emerging Micro-Electric-Mechanical-System and nano-cryosurgery, freezing of the micro liquid droplet has aroused increasingly public concern. Instead of using conventional mechanical valve, the ice valve was recently developed to work in the microfluidics by way of freezing or melting of the liquid [8].

Freeze tweezer was proposed to manipulate micro object using nucleotide ice [9]. The spray-freezing process, which was developed for powder production, has been also fully investigated through studies on atomized liquid droplets freezing.

In fact, during the past few decades, many ever-developing experimental techniques have been carried out as potent assistants for characterization of the solidifying process. Various types of cryo-microscopes were designed to observe the freezing behaviors under different conditions [10–12]. Component stages of nucleation and crystal growth were both depicted definitely. Raman spectroscopy was used to study the formation of ice lenses in porous medium freezing [13], because a molecular-optic band peak at 225 cm^{-1} will increase in the Raman spectrum if ice exists. Moreover, the cryogenic transmission electron microscopy technique also works by providing more detailed information not accessible by other ways [14]. Since understanding the phenomenology of spray crystallization was important to determine which parameter contributed, the imaging technology therefore became one of the most effective ways for detail observation. The liquid fraction data of the droplet obtained by nuclear magnetic resonance (NMR) spectrometry were favorable on verification of the numerical predictions [15]. Anisotropic self-diffusion in salt water ice could be also presented by NMR imaging [16]. The magnetic resonance imaging mapping demonstrated that the supercooling and the heat transfer rate would relate to the final microstructure of freezing droplet [17]. Except for the above imaging ways, thermal analysis was also frequently adopted for characterizing the phase transition within water droplet and the related supercooling problems [18, 19].

However, the currently available experimental systems are either too complex to construct, or too reliant on diagrams to illustrate directly. It is still not convenient enough for the in situ observation, especially when the volume of the liquid is quite small. In addition, to quantify the total freezing time, recording the droplet temperature was indispensable. Owing to the special characteristics that may exhibit by the micro droplet during freezing, the temperature curves monitored were demonstrated as a new strategy for evaluation of the biological viability [20]. However, the temperature measurement has to insert a thermocouple into restricted space, which will definitely destroy the micro environment during the practical freezing process. Therefore, a non-invasive method for characterizing the freezing behavior of a liquid droplet was urgently waiting for establishment.

Objective

This study is aimed to set up a new method, which uses the infrared (IR) thermovision technology, to fulfill the tasks of both the direct imaging and the temperature recording of the micro liquid droplet subject to freezing. Instant of the occurring phase change was on a chance of being captured by the visual color break in IR images. Approach proposed here is expected to be of significance in achieving visualization of phase change moment via a non-contact style, which may be utilized in freezing detection at micro/nano scale in many related areas.

Experimental

Materials

The materials referred in the experiments included the distilled water, the 10% (v/v) solution of aqueous dimethylsulfoxide (DMSO), and the 0.2% (w/w) suspension of Fe_3O_4 nano-particles (NPs) with an average diameter of $\sim$20 nm. Sample droplets were placed on a cover slip sequentially by the micro-syringe of 1 and 10 µl, which had the droplet size deviation of 0.02 and 0.2 µl, respectively. Heat conductive silicone was sandwiched between the cover slip and the top copper for better contact. In order to ensure the experimental conditions constant, the substrate cover slip was cleaned by ethanol and deionized water between experiments on the same liquid, and replaced between different liquids.

Methods

Test apparatus and primary procedures

The whole system was consisted of four main apparatus: (a) the freezing stage; (b) the IR thermograph ThermaCAM A40 camera, developed by FLIR Company (USA), with wavelength range within 8–14 µm and temperature resolution of 0.08 °C; (c) the computer for data acquisition; and (d) the power supply source. The sample freezing was achieved by the freezing stage, which was configured in two-staged thermoelectric (TE) modules (as described in Fig. 1). The first stage consisted of two 15 mm × 30 mm TE modules acting as the heat sink for two additional 15 mm × 15 mm modules mounted on its top as the second stage. The intermediate and top copper plates were fixed on upper surface of each stage, respectively, in order to improve the cooling performance. The hole drilled at the center was used for direct microscopy observation. The cooling chamber confining the circulation of the cooling water was settled at the bottom of the first stage to take away the heat generated by the TE modules. As substitute of the universal fan and fins for heat dissipation, the water-cooling chamber effectively avoided unwanted vibration caused by the kinetic component. The whole stage will

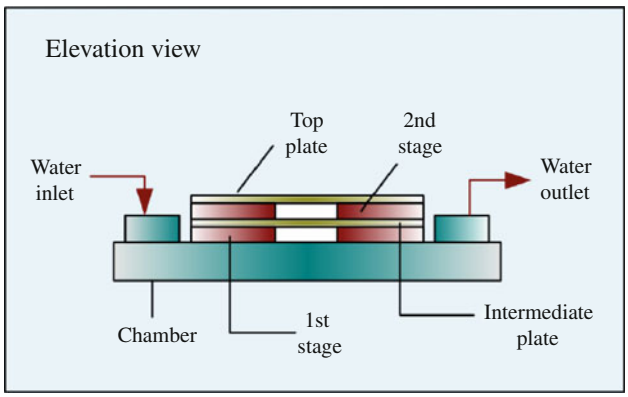

Fig. 1 Elevation section of the thermoelectric freezing stage

initiate freezing after switching on the electricity supply, and if needed, can be used as a heater by changing direction of the electric current in the circuit. The dynamic IR thermography was collected by the ThermaCAM^{TM} A40 camera. The objective temperature distribution could thus be calculated from the IR images according to specific formulas. This technology has been used to depict the freezing of the large block water and its accompanying natural convection [21, 22].

Once the test began, samples would be loaded on the freezing stage and cooled from the room temperature until completely frozen. Under condition of 1.97 A electric current supplied, the stage worked at the approximately maximum rate as allowed. The phase change process was recorded by the video at the highest speed, which consisted of a series of IR photographs taken at every tens of microseconds. Accuracy of the images was guaranteed by right settings of the camera parameters and focus distance. Meanwhile, the data collected were transmitted to the computer and further analyzed by the accessorial software ThermaCAM^{TM} Researcher.

Geometrical shape of the droplet resting on the substrate

The shape of the droplet rested on the substrate does matter the temperature distribution, the evaporation rate, and the future freezing process. Unlike the single bead suspended in the air, not only the properties of the droplet itself are involved, but also the surface characteristics of the substrate are regarded as the key factors. Balance of the multi-effects, such as the surface tension, the gravity, the viscosity, the surface roughness of the substrate, etc., poses the steady state geometrical shape of the droplet.

For small water droplet on the glass, the assumption of shape formation of spherical cap was demonstrated valid according to specific computation of the Bond and capillary numbers. The typical geometrical shape of droplet we adopted was illustrated in Fig. 2 to support the assumption.

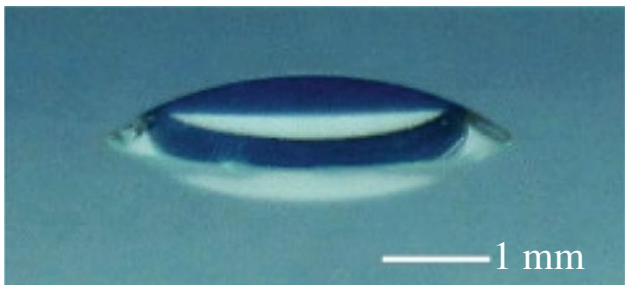

Fig. 2 Geometrical shape of 5 μl water droplet on the glass cover slip

The radius and height of the droplet were estimated as 4 and 1 mm. The contact angle with glass slip was approximately estimated as 37° by taking picture of the droplet from different directions via high quality digital camera and then doing a calculation. However, once the substrate changed, no matter what is the material or the roughness, the geometrical sizes of the droplet may be unavoidably different, as well as its final shape. Therefore, it is of great significance to keep constant conditions in repeated experiments.

Test verification

Setting suitable parameters for the IR camera is quite important to guarantee accuracy of the acquired images. Three primary effects that cannot be ignored are IR emissivity of the objective, the reflected radiation in the object from the surroundings, and the radiation loss due to atmospheric absorption along the light way. The emissivity, which is defined as the ratio of the emissive radiation from the objective to that from the perfect blackbody, is the most critical parameter to be set correctly. In order to validate the setting, a thermocouple was employed for comparison with result of the IR camera. If the error between each other cannot be ignored, the emissivity setting will be modified until the same temperature as measured by thermal couple can be obtained. Considering that the phenomena, we concerned included process of frost and droplet freezing, the emissivity of the objective was finally evaluated as an average value of 0.97 [23, 24].

Results and discussion

IR thermography

The presentation of the results will begin with the display of the IR images of the micro droplet during freezing. The volumes of the experimental droplets are restricted to 1, 5, and 10 μl, respectively. As demonstrated in [25], the ideal physical process of a droplet freezing can be described as experiencing four stages. First, the liquid droplet is

supercooled to below the equilibrium freezing point (EFP) at the pre-cooling stage. Then, it is subjected to the recalescence stage, when the crystal began to grow rapidly. Once the temperature reaches the EFP, the droplet would step into the freezing stage. The stage ends until the droplet is completely frozen. After that, the temperature of the solid droplet descends at the final cooling stage. Experiments in this passage are dedicated to realize the visualization of the four freezing stages by IR camera for the first time. In particular, the instant recalescence stage is expected to be captured on the basis of the involved temperature jump.

The first experiment was performed on the distilled water. Freezing evolution of a droplet at 5 μl was illustrated in Fig. 3. Clearly, supercooling state of the droplet could be observed distinctly in the images. Since the freezing stage was exposed to the environment, steam in air was condensed into water, when it touched the cold surface of the cover slip, then converted to frost after being supercooled enough. During the whole investigation, the accompanying frost phenomenon was not eliminated as intruder for two reasons. On the one hand, it was of extreme difficulties to keep the surrounding air desiccant while simultaneously preserve the micro droplet from vaporization. On the other hand, the frost phenomenon not only produced little effect on the problem we concerned, but also can act as a reference of initiation of water freezing. As indicated, frost came into being in Fig. 3a. Evident temperature enhancement could be observed wreathing the objective droplet as shown in Fig. 3b, which was attributed to the latent heat release as a result of bead frosting on the cover slip. Recalescence stage of the objective droplet was approved according to the color break as index of temperature elevation induced by nucleation effect as Fig. 3c. Once the moment ended, the droplet temperature would gradually descend from the edge to the center as shown in Fig. 3d.

The second experiment was performed on the DMSO solution. As is well known, cryopresevation is regarded as the most promising way for long-term storage of biological samples. Many methods have been designed to optimize the practical process. Addition of the cryoprotective agent is one of the most effective techniques adopted under certain optimal cooling programs. DMSO is such a kind of cryoprotective agent to keep biological tissues from being functionally destroyed. As revealed in Fig. 4, the droplet was not frozen at the same time when frost appeared deviating with pure water. The reason was attributed to its freezing prevention effect, which can be illustrated by IR images convincingly. However, it does not mean that the DMSO droplet will never be completely frozen. The freezing point of the solution deeply depends on its volume concentration.

The subsequent experiment was performed on the Fe_3O_4 NPs suspension due to increasing concerning on the freezing mechanism while NPs were added. The reason to choose Fe_3O_4 NPs was taking account of the biological comparability in practical applications. It was noteworthy that the mixture should be dealt by ultrasonic vibration for more than 3 h to ensure the uniformity of the NPs distribution. The IR images of NPs droplet were not given here, since results obtained were similar to that of pure water on nucleation temperature when freezing began, although uniformity and concentration of the NPs were believed to be influential to specific phenomena according to heterogeneous nucleation theory. However, details could refer to

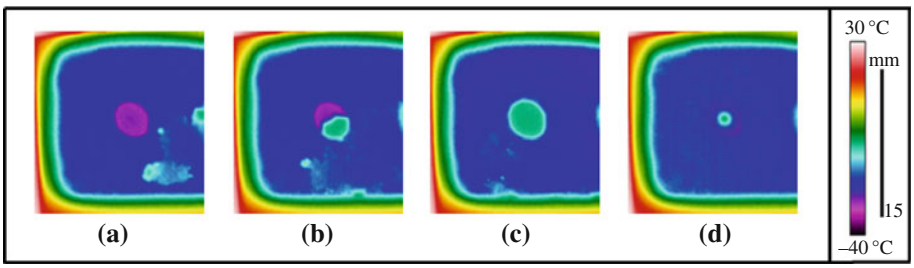

Fig. 3 Infrared mapping of the distilled water droplet at 5 μl during freezing phase change. The time of each image is specified as **a** $t = 104.9$ s, **b** $t = 105.1$ s, **c** $t = 105.2$ s, **d** $t = 111.3$ s

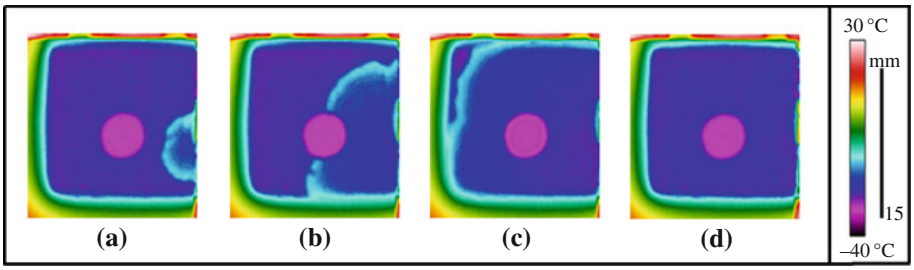

Fig. 4 Infrared mapping of the DMSO solution droplet at 5 μl during freezing phase change. The time advance of every image is specified as **a** $t = 72.7$ s, **b** $t = 72.7$ s, **c** $t = 72.9$ s, **d** $t = 73.6$ s

explanations about pure water. Moreover, results here may raise more concerns on the zero size effect of the particles, which has ever been revealed as disappearance of the particle effects in favor of nucleation as believed in classical theories.

Freezing curves and data analysis

Although the previous experiments have provided a preliminary demonstration of the validity of using IR thermograph to map freezing of the micro liquid droplet, some more critical factors, such as the droplet sizes, the freezing rate of the TE modules, the surface tension of the droplet on the cover slip, etc., will also influence the process. In order to overcome these troubles, the new measurement was carried out for exact data analysis. 3 μl droplets of distilled water, DMSO solution, and NPs suspension were placed on the cooling surface simultaneously. The placement of the droplets was ensured to be as close as possible, so that uncertainty owing to the spatial arrangement was eliminated.

Figure 5 illustrated the real-time temperature curves of various materials. The monitored spots 1–3 were localized in the center of the surface of the distilled water, the NPs suspension, and the DMSO solution, respectively. Four typical stages as mentioned in the last section were examined and certified in Fig. 5a. Considering that the second and third stages were so instantaneous, the details were revealed in Fig. 5b. One can observe that, for the former two kinds of droplets, the temperature jumped at stage ② from the supercooling state to the EFP and kept constant 0 °C for about 2 s during stage ③. However, for the DMSO droplet, curve of temperature break at stage ② was not as sharp as the former ones. The cryoprotective agent not only delayed the droplet freezing, but also weakened the release of the latent heat at the phase change moment. However, according to results of the repeated experiments, it was of urgent need to point out that, for pure water and NPs suspension, the emergent time sequence of the temperature jumps at stage ② and the durative times of the stage ③ were somewhat random. The lack of reproducibility does relate to the freezing rate and freezing time. Without regard to the tiny uncontrollable environmental influence, the reason was assumed to correlate with change of the contact angle between different droplets, which is induced by uniformity difference of the NPs as result of unavoidable NPs aggregation with time.

Figure 6 showed more details on spatial temperature profiles for the micro droplets during the phase change process. As depicted in Fig. 6a, three metrical straight lines with the same length were plotted across the droplets 1–3, which represented the distilled water, the NPs suspension, and the DMSO solution, respectively. Temperature distributions along the lines at five different moments were given in Fig. 6b–f. Here, "Row numbers" represents spatial horizontal coordinates along the lines of 1–3, as depicted in (a), respectively. The specific number in fact indicates a relative position which is automatically displayed as pixel of thermograph image by the camera software. This value can be correlated with the actual size of the droplet through careful size calibrations. In Fig. 6, considering that the core issue is to disclose with generalized purpose the transient temperature distribution of the droplet along line 1, 2, or 3 and thus to evaluate its global phase change image, only relative coordinate was provided on the picture for clarity. Fig. 6b was collected before recalescence. Obviously, temperature of the droplet surfaces along the lines were uniformly distributed and approximate 11–12 °C supercooling was suffered by the micro droplets. Figure 6c, d were captured at the moment when the first and second nucleation process happened. Distinctly, droplet temperature of the NPs suspension and the distilled water began to jump to 0 °C of time sequencing. Fig. 6e illustrated the phase change of the DMSO droplet, as well as the initial period of the other droplets, when temperature decayed from the edge after nucleation. The EFP of the DMSO was established as −6 °C, which was lower than the distilled water under the same conditions. When the freezing stage ended, the droplets began to be cooled again from their own EFPs.

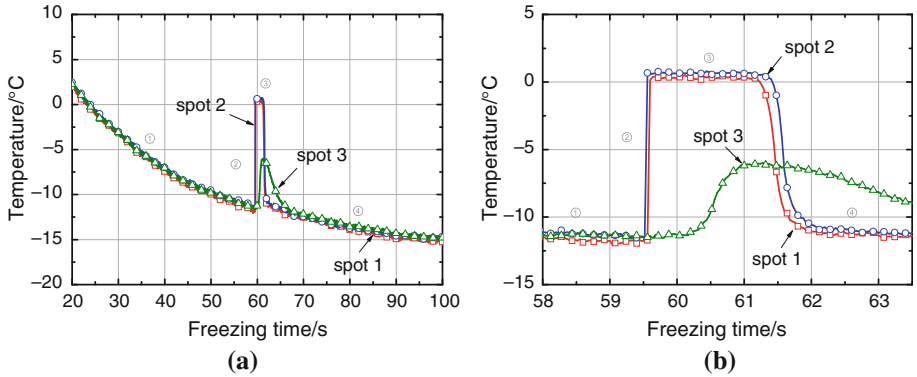

Fig. 5 Diagram of the surface temperature variation of the 3 μl droplets during freezing. **a** Shows the intact temperature curves of different droplets subject to freezing; **b** shows the temperature details during the second and third freezing stages. Four typical stages are specified as ① the supercooling stage, ② the recalescence stage, ③ the freezing stage, and ④ the cooling stage

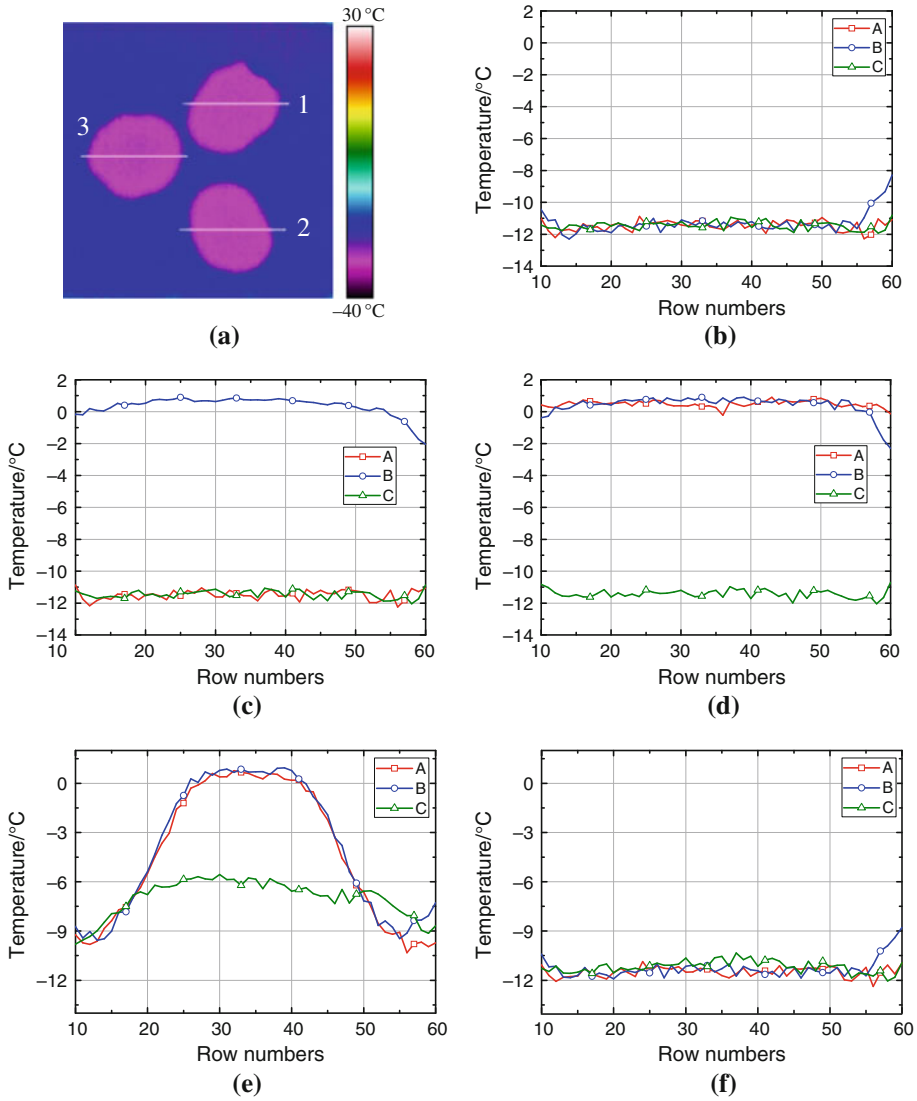

Fig. 6 Spatial temperature profiles for the micro droplets during the phase change process at different moments. **a** Shows locations of three measuring lines. The moments of (**b**)–(**f**) are specified as: **b** $t = 59.4$ s, **c** $t = 59.6$, **d** $t = 59.6$ s, **e** $t = 61.0$ s, **f** $t = 65.3$ s. In (**b**)–(**f**), A, B, C indicate temperature distributions along lines 1–3 in (**a**), respectively; "Row numbers" represents relative spatial horizontal coordinates along the lines of 1–3, as depicted in (**a**), respectively

Figure 6f showed the droplet temperature subject to the cooling stage, while the temperature came back to the beginning of the phase change moment.

Nucleation temperature and types of the solidification

In this study, the droplet cooling was achieved by a conductive way as substitute of the convective methods, which was widely used in the experimental investigations of the plasma spray processes. The reason why the flat substrate but not the cold air, was introduced to be as the heat sink of the freezing droplet was taking into account the demand of both the IR thermograph for visibility and avoidance of the droplet evaporation. The direct contact between the droplet and the substrate impacted much on the nucleation mechanism and the initial frozen fraction. Therefore, it was extremely pivotal to understand the effects of their interactions.

Different ways of nucleation will determine both the nucleation temperature and type of the freezing occurring. In terms of whether there exist foreign bodies or not, the nucleation is usually classified as homogeneous or heterogeneous cases. It is no doubt that once the substrate is involved, the nucleation process definitely belongs to the latter one. Compared with the nucleation in the homogeneous case, the nucleation point of pure water will be elevated much due to the increasing amount of nucleation embryos introduced by foreign bodies. In this study, the nucleation temperature was ascertained about −12 °C from experimental results. It was much higher than −40 °C where homogenous nucleation would happen. From viewpoint of thermodynamics, occurrence of the glass flat substrate would lower the nucleation barrier effectively, so that difficulties of nucleation and solidifying were reduced.

On the other hand, whether a substrate exists would act as a factor on types of the occurring solidification. As one

knows, freezing initiates at the location where the ice embryo firstly formed. For a single droplet, the direction of solidifying is supposed to have two possible choices. If no substrate disturbs, the ice will nucleate at the surface and propagate inwardly from the frozen ice shell. Otherwise, the nucleation will be localized originally at the substrate. Typical instance comes that, when junction of the thermocouple is included in the center, the droplet will be frozen outwardly from the central ice embryo. Impacts of different freezing types will involve position tracing of the solid–liquid interface, as well as the freezing time related. Therefore, the flat substrate employed in our experiments attached itself to raising the nuclei and the upward freezing. That was the reason why the water droplet seemed to be frozen from the edge to the center during the third stage as recorded by IR camera.

Initial frozen volume produced from the recalescence

Recalescence phenomenon is usually depicted as the abrupt temperature rise due to release of the latent heat during liquid freezing. For the bulk fluid, the degree of supercooling is so small that such phenomenon is not easy to be detected consequently. However, for the liquid droplet, the generally larger supercooling makes it possible to be captured as indication of the phase change. Although the recalescence occurs always extremely rapidly, the initial frozen volume is produced significantly making sense on accurate prediction of the total freezing time. If assumption of no time duration in recalescence stage is made, the initial frozen volume V_f can be estimated by the energy balance, expressed as [26]

$$V_f = f_s V_d = \frac{\rho_l c_l (T_f - T_n)}{\rho_s \quad L_f} V_d, \tag{1}$$

where f_s is the solid fraction; V_d is volume of the droplet; ρ_l, ρ_s are density of the liquid and solid; c_l is the specific heat capacity of the liquid; T_f, T_n represent the equilibrium freezing temperature and the nucleation temperature, respectively; L_f is the latent heat of freezing phase change. Sometimes, once there is no need to compensate for the density difference between the liquid and solid, the solid fraction would be simplified as the defined Stefan number (St) [27]

$$St = f_s = \frac{c_l (T_f - T_n)}{L_f}. \tag{2}$$

Obviously, f_s was dependent on the nucleation temperature, but independent of the droplet volume. As for water, the variation of the physical properties with temperature could be calculated by the following equations [28, 29].

$$\begin{aligned} c_l &= -0.0011T^3 + 0.732T^2 - 163T + 16582 \\ \rho_l &= -0.02T^2 + 10.8T - 470 \\ \rho_s &= -0.163T + 961.4. \end{aligned} \tag{3}$$

As illustrated in Eq. 1, the solid fraction would be reduced with the temperature increasing through a quasi-linear way along, and calculated as 0.168, when real experimental nucleation temperature was identified as −12 °C.

Conclusions

In this study, the IR thermography technology was validated for recording the freezing phase change process of the micro liquid droplet, which opens its possibility of being extended as a new conceptual differential scanning calorimetry in the near future. Four classic solidifying stages were directly depicted by IR images, especially the recalescence phenomenon, which was always regarded as initiation of the phase change. Specific temperature data were picked up and differences exhibited by the DMSO droplet was attributed to the demonstrated cryoprotective effect. Meanwhile, the effects introduced by the flat substrate were investigated generally for better understanding. The initial frozen fraction was calculated to be 0.168 at the experimental nucleation temperature, which acted as the crucial factor to determine the total freezing time. However, due to restrictions of the experimental conditions, as well as the influence of the concentration and uniformity, no evident difference of the NPs suspension was observed. More details on this issue need further studies in the near future.

Acknowledgements This study was partially supported by the Specialized Research Fund for the Doctoral Program of Higher Education, the NSFC, and Tsinghua-Yue-Yuen Medical Sciences Fund.

References

1. Zuberi B, Bertram AK, Cassa CA, Molina LT, Molina MJ. Heterogeneous nucleation of ice in $(NH4)_2SO_4$–H_2O particles with mineral dust immersions. Geophys Res Lett. 2002;29:1421–4.
2. Knight CA. Ice nucleation in the atmosphere. Adv Colloid Interface Sci. 1979;10:369–95.
3. Hills BP, Goncalves O, Harrison M, Godward J. Real time investigation of the freezing of raw potato by NMR microimaging. Magn Reson Chem. 1997;35:S29–36.
4. Zachariassen KE, Kristiansen E. Ice nucleation and antinucleation in nature. Cryobiology. 2000;41:257–79.
5. Fletcher NH. On ice-crystal production by aerosol particles. Meteorol J. 1959;16:173–80.
6. Liu XY. In: Sato K, Furukawa Y, Nakajim K, editor. Advances in crystal growth research. Amsterdam: Elsevier Science Publishers B.V.; 2001. p. 42–8.

7. Mazur P, Leibo P, Chu EH. A two-factor hypothesis of freezing injury: evidence from Chinese hamster tissue-culture cells. Exp Cell Res. 1972;71:345–55.
8. Yang Y, Liu J. Numerical stimulation on operating process of ice valve for controlling micro/nano fluidics. Chin J Sens Actuators. 2006; 19:2022–24 (In Chinese).
9. Yang Y, Liu J. Numerical simulation on operating process of freeze tweezer for manipulation of micro/nano objects. Chin J Sens Actuators. 2006; 19:1673–76 (In Chinese).
10. Diller KR, Cravalho EG. Cryomicroscopic investigation of intracellular ice formation in frozen erythrocytes. Cryobiology. 1971;8:398–406.
11. Namperumal R, Coger R. A new cryostage design for cryomicroscopy. J Microsc. 1998;192:202–11.
12. Petersen A, Schneider H, Rau G, Glasmacher B. A new approach for freezing of aqueous solutions under active control of the nucleation temperature. Cryobiology. 2006;53:248–57.
13. Watanabe K, Mizoguchi M. Ice configuration near a growing ice lens in a freezing porous medium consisting of micro glass particles. J Cryst Growth. 2000;213:135–40.
14. González-Pérez A, Olsson U. Cryo-fracture TEM: direct imaging of viscous samples. Soft Matter. 2008;4:1625–9.
15. Hindmarsh JP, Wilson DI, Johns ML, Russell AB, Chen XD. NMR verification of single droplet freezing models. AIChE J. 2005;51:2640–8.
16. Menzel MI, Han SI, Stapf S, Blümich B. NMR characterization of the pore structure and anisotropic self-diffusion in salt water ice. J Magn Reson. 2000;143:376–81.
17. Hindmarsh JP, Buckley C, Russell AB, Chen XD, Gladden LF, Wilson DI, Johns ML. Imaging droplet freezing using MRI. Chem Eng Sci. 2004;59:2113–22.
18. Kousksou T, Jamil A, Gibout S, Zeraouli Y. Thermal analysis of phase change emulsion. J Therm Anal Calorim. 2009;96:841–52.
19. Nitsch K. Thermal analysis study on water freezing and supercooling. J Therm Anal Calorim. 2009;95:11–4.
20. Liu J, Zhou YX. Freezing curve-based monitoring to quickly evaluate the viability of biological materials subject to freezing or thermal injury. Anal Bioanal Chem. 2003;377:173–81.
21. Błogowska K, Domański R. Noninvasive measurement of temperature field in natural covection of solidifying saline water. In: Proceeding of the 3rd IASME/WSEAS international conference on heat transfer, thermal engineering and environment. Corfu, Greece; 2005. p. 35–38.
22. Wisniewski TS, Kowalewski TA, Rebow M. Infrared and liquid crystal thermography in natural convection. In: 8th International symposium on flow visualization. Edinburgh; 1998. p. 212.1–8.
23. Bramson MA. Infrared radiation: a handbook for applications. New York: Plenum Press; 1968.
24. Wolfe WL, Zissis GJ. The infrared handbook. Washington: Office of Naval Research, Department of the Navy; 1978.
25. Hindmarsh JP, Russell AB, Chen XD. Experimental and numerical analysis of the temperature transition of a suspended freezing water droplet. Int J Heat Mass Trans. 2003;46:1199–213.
26. Hu H, Larson RG. Evaporation of a sessile droplet on a substrate. J Phys Chem B. 2002;106:1334–44.
27. Hindmarsh JP, Wilson DI, Johns ML. Using magnetic resonance to validate predictions of the solid fraction formed during recalescence of freezing drops. Int J Heat Mass Trans. 2005;48:1017–21.
28. Kucherov AN. Sublimation and vaporization of an ice aerosol particle in the form of thin cylinder by laser radiation. Int J Heat Mass Trans. 2000;43:2793–806.
29. Gao W, Smith D, Sego D. Freezing behavior of freely suspended industrial waste droplets. Cold Regions Sci Technol. 2000;31:13–26.